Radiocarbon, Vol 62, Nr 1, 2020, p 235–242 DOI:10.1017/RDC.2019.113

SPATIAL DISTRIBUTION OF ^{14}C IN TREE LEAVES FROM BALI, INDONESIA

Tamás Varga[1*] • A J Timothy Jull[1,2,3] • Zsuzsa Lisztes-Szabó[1] • Mihály Molnár[1]

[1]Isotope Climatology and Environmental Research Centre, Institute for Nuclear Research, Hungarian Academy of Sciences (ATOMKI), Debrecen, H-4001, P.O. Box 51, Hungary
[2]Department of Geosciences, University of Arizona, Tucson, AZ85721, USA
[3]University of Arizona AMS Laboratory, Tucson, AZ85721, USA

ABSTRACT. The increase of fossil-fuel-derived CO_2 in the atmosphere has led to the dilution of the atmospheric radiocarbon concentration, but due to the costly instrumentation, the continuous atmospheric $^{14}C/^{12}C$ data is incomplete in developing countries, such as in Indonesia. These data give useful information about the level of local and regional fossil emissions. In this study, ^{14}C AMS measurements of local vegetation and woody plant species samples have been used to estimate the rate of fossil-fuel-derived carbon in the plants, which fix the CO_2 from the atmosphere by photosynthesis. Evergreen leaf samples were collected in September 2018 on the island of Bali in different, diverse districts in local and urban areas. The samples from the densely populated areas show observable fossil fuel emissions and show that the $\Delta^{14}C$ level is close to zero ‰, similar to the natural level.

KEYWORDS: AMS, CO_2, evergreen, fossil carbon, leaf.

INTRODUCTION

Natural and anthropogenic carbon sources and sinks affect the radiocarbon concentration in the atmosphere at the same time. These effects affect the $^{14}C/^{12}C$ ratio both at a local and global scale (Graven et al. 2015; Major et al. 2018). The main anthropogenic sources are radiocarbon production from nuclear reactions, such as nuclear weapons testing and the nuclear energy industry. Nuclear bomb tests doubled the natural ^{14}C level in the atmosphere from the late 1950s to early 1960s (Nydal and Lövseth 1983; Buzinny 2006). This radiocarbon level (known as the "bomb spike") is decreasing and now is close to the natural, preindustrial or pre-bomb level due to exchange between the terrestrial and oceanic reservoirs and the dilution effect of the addition of fossil-fuel carbon to the atmosphere. The second anthropogenic source is the burning of fossil fuels producing radiocarbon-free greenhouse gases, such as CO_2 (Suess 1955). These fossil fuels and materials do not contain radiocarbon due to the 5700 ± 30 yr half-life of ^{14}C and long-term geological storage (Bella et al. 1968; Levin et al. 2010; Berhanu et al. 2017; Varga et al. 2018). The natural sources of radiocarbon are the production of ^{14}C in the troposphere by the $^{14}N(n,p)^{14}C$ reaction (McNeely 1994; Povinec et al. 2017) due to cosmic radiation and intensive cosmic events. There are other natural sources that do not cause the enrichment of radiocarbon but can dilute the radiocarbon concentration, such as magmatic or volcanic sources that emit radiocarbon-free carbon to the atmosphere (Shore and Cook 1995; Cook et al. 2001). Plants fix the CO_2 from the atmosphere by photosynthesis, so plant materials, such as leaves and tree rings, can be a method of biomonitoring the atmospheric radiocarbon concentration (Pawelczyk and Pazdur 2004; Pazdur et al. 2007; Quarta et al. 2007; Rakowski 2011; Janovics et al. 2013, 2016). Evergreen species are often avoided for this reason but in the tropical regions deciduous trees are less common, so in this study, only evergreen leaf samples were collected as a biological record of atmospheric radiocarbon concentration (Alessio et al. 2002). Samples were collected at 13 sampling points in Bali, Indonesia, close to urban activity and traffic, and far from roads and intensive industry. The samples were prepared and measured by MICADAS type accelerator mass spectrometer (AMS) at the Hertelendi Laboratory of Environmental Studies (HEKAL), Hungary, Debrecen (Synal et al. 2007; Molnár et al. 2013). The primary aim of the study was to give

*Corresponding author. Email: varga.tamas@atomki.mta.hu.

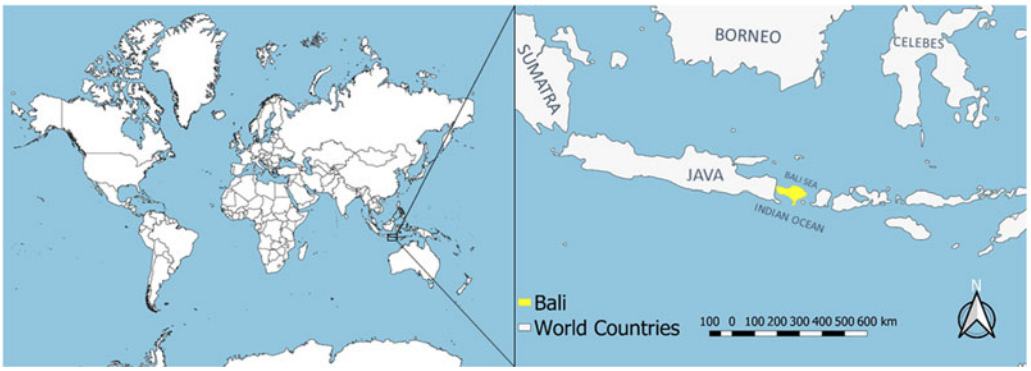

Figure 1 Location of Bali Island.

an overview of the radiocarbon distribution of Bali island and supplement the incomplete radiocarbon information about this region.

METHODS

Sampling Sites

Bali island is part of Indonesia, located east of Java. The population of Bali province is more than four million people. The provincial capital and most populated city is Denpasar. The island is the most popular tourist destination in Indonesia and tourism is the leading contributor to economy (Rahayu et al. 2018). The climate of the island has typical Asian-Australian monsoon seasonality with dry and wet seasons (Fukumoto et al. 2015). The vegetation is mainly evergreen due to the tropical climate. The location of Bali Island is shown in Figure 1. During the sampling campaign, in total, samples of woody plants (tree) leaves were collected at 13 sampling points around the Bali Island (Table 1). The samples, fresh leaves from the end of the branches were collected from different districts, forested areas, rice paddies, and urban vegetation close to busy crossroads as well as urban background areas. A minimum 3 pieces of tree leaves were collected from 180 cm high to determine the local fossil carbon load. Taxon names are listed based on the International Plant Name Index (IPNI 2019).

SAMPLE PREPARATION AND MEASUREMENT

The collected plant materials were kept frozen until chemical preparation. The samples were cut into small pieces, then homogenized before pretreatment. The standard acid-base-acid preparation protocol was used for the purification of the samples (Southon and Magana 2010), subsequently, the samples were dried in a heating block at 50ºC. The dried samples were combusted in sealed glass tubes at 550ºC for 12 hr, using MnO_2 as an oxidant to convert the carbon of organic material to CO_2 (Janovics et al. 2018). The liberated CO_2 gas was purified from H_2O and different contaminants in a dedicated vacuum line. The pure CO_2 gas was trapped in glass tubes (with Zn, TiH catalysts and iron powder) sealed by flame and converted to graphite following the sealed tube graphitization method (Rinyu et al. 2013). After graphitization, the graphite samples were pressed into aluminium targets for the accelerator mass spectrometry (AMS) measurements to determine the carbon isotopic composition of the plant samples (Molnár et al. 2013). For data evaluation, "Bats" data reduction software was used (Wacker et al. 2010). For the reporting of ^{14}C data, pMC and $\Delta^{14}C$ units were used (Stuiver and Polach 1977; Stenström et al. 2011).

https://doi.org/10.1017/RDC.2019.113 Published online by Cambridge University Press

Table 1 Sampling location and species of plant samples.

Nr (#)	Area description	Latitude	Longitude	Species of tree
1	Urban background	–8.6052	115.2501	*Ficus elastica* Roxb.
2	Urban background	–8.5182	115.2585	*Micromelum minutum* (G. Forst.) Wight & Arn.
3	Rice field	–8.4279	115.2797	*Altingia poilanei* Tardieu
4	Urban area, parking place	–8.2772	115.3512	*Diospyros celebica* Bakh.
5	Urban background	–8.6193	115.0869	*Ficus elastica* Roxb.
6	Rice field	–8.3706	115.1353	*Ficus septica* Burm f.
7	Urban background	–8.275	115.1666	*Citrus aurantium* L.
8	Urban background	–8.544	115.1722	*Avicennia officinalis* L.
9	Crossroads	–8.7905	115.2125	*Ficus fistulosa* Reinw. ex Blume
10	Crossroads	–8.7936	115.2155	*Ficus obliqua* G. Forst.
11	Urban background	–8.8322	115.0862	*Celtis rigescens* Planch.
12	Urban background	–8.7934	115.2291	*Citrus aurantium* L.
13	Parking place of the airport	–8.7427	115.1649	*Diospyros celebica* Bakh.

For the environmental samples we use $\Delta^{14}C$ units:

$$\Delta^{14}C = \left(\frac{A_{SN}}{A_{ABS}} - 1\right) \quad 1000\,‰ \quad \text{(without age correction)} \tag{1}$$

Where A_{SN} is the stable isotope normalized specific radiocarbon activity of the samples, and A_{ABS} is the specific activity of the absolute radiocarbon standard (226 Bq/kg carbon) (Stenström et al. 2011).

Fossil Contribution

For all the measured samples, the fossil-fuel-derived CO_2 ratio (F) and fossil fuel CO_2 component (CO_{2ff}) was calculated by the following equations (Levin et al. 2003):

$$F = \frac{\Delta^{14}C_{bg} - \Delta^{14}C_{meas}}{\Delta^{14}C_{bg} + 1000\,‰} \tag{2}$$

Where $\Delta^{14}C_{bg}$ is the radiocarbon content of the background sample, $\Delta^{14}C_{meas}$ is the radiocarbon content of the measured sample (Baydoun et al. 2015). In our case, the $\Delta^{14}C_{bg}$ is represented by the sample with the highest measured radiocarbon content, due to the lack of proper local background atmospheric $^{14}CO_2$ measurements, the highest $\Delta^{14}C$ value represents the lowest fossil carbon content.

$$CO_{2ff}(ppmv) = \frac{CO_{2meas}\left(\Delta^{14}C_{bg} - \Delta^{14}C_{meas}\right)}{\Delta^{14}C_{bg} + 1000\,‰} \tag{3}$$

Where $\Delta^{14}C_{bg}$ is the radiocarbon content of the background sample, $\Delta^{14}C_{meas}$ is the radiocarbon content of the measured sample, CO_{2meas} is the measured CO_2 content in the

https://doi.org/10.1017/RDC.2019.113 Published online by Cambridge University Press

Table 2 Summary of ^{14}C results taken at different sampling districts of Bali, Indonesia.

Nr. (#)		pMC	±	$\Delta^{14}C$	±	F (%)	±	CO_{2ff} (ppmv)	±
1		101.6	0.5	7.5	4.6	1.1	0.6	4.3	2.5
2		101.9	0.5	10.9	4.6	0.7	0.6	2.9	2.5
3*		102.7	0.5	18.2	4.6	0.0	0.6	0.0	2.5
4		100.9	0.5	0.9	4.5	1.7	0.6	6.9	2.5
5		101.7	0.4	9.1	4.5	0.9	0.6	3.7	2.5
6		102.0	0.5	11.8	4.6	0.6	0.6	2.6	2.5
7		101.8	0.5	9.3	4.6	0.9	0.6	3.6	2.5
8		101.9	0.5	10.5	4.6	0.8	0.6	3.1	2.5
9		98.0	0.4	–28.2	4.4	4.6	0.6	18.6	2.4
10		96.2	0.4	–46.0	4.3	6.3	0.6	25.8	2.4
11		102.6	0.5	17.4	4.6	0.1	0.6	0.3	2.5
12		101.7	0.5	8.6	4.5	1.0	0.6	3.9	2.5
13		100.8	0.5	–0.7	4.5	1.9	0.6	7.6	2.5
Mean	Scatter	101.1	1.9	2.2	18.6	1.6	1.8	6.4	7.5

*The sample with the highest measured radiocarbon content ($\Delta^{14}C_{bg}$).

atmosphere at the time of sampling (Berhanu et al. 2017). In this study, the CO_{2meas} is represented by the annual CO_2 concentration (ppm) in 2018 at Mauna Loa, Hawaii, 408.5 ppm (NOAA 2019).

Based on these calculations, the fossil carbon contribution can be estimated in the air and indirectly in the vegetation.

RESULTS AND DISCUSSION

The differentiation of the $\Delta^{14}C$ data of evergreen plant samples is not simple, because the growing season is not as well-defined, as the case of deciduous species. Due to this situation, the comparison to atmospheric $^{14}CO_2$ data is not the same for every sample, because some leaves may have created at different time and the evergreen leaves may store fixed carbon from previous years (Pataki et al. 2010). For this reason, we compared our results to each other and the local "background" to identify the most radiocarbon depleted areas. Table 2 lists the results of AMS measurements of plant samples. The highest $\Delta^{14}C$ data, equal to or greater than 11.8‰ were measured at the sampling point no. 3, 6, and 11. These sampling points were at rice fields (no. 3 and 6) and an urban background area on the southern coast (no. 11). These areas were relatively distant from direct urban CO_2 emissions and industrial facilities, a minimum 100 m away from roads. Although the longevity of evergreen leaves can be more than one year (Ewers and Schmid 1981), in our case, only fresh leaves were collected.

The average $\Delta^{14}C$ value is 2.2‰ but the scatter is ± 19‰ in case of 13 sampling point. There are two higher values, which are samples taken from urban districts, close to busy crossroads with heavy traffic at sampling points no. 9 and 10. Furthermore, there are two relatively lower $\Delta^{14}C$ data at sampling points no. 4 and 13 from different parking places of a tourist attraction and the airport of Denpasar. The most polluted area was a crossroad (no. 10) where the traffic is moderated by a traffic light with a long waiting time for cars and scooters. This has the result

https://doi.org/10.1017/RDC.2019.113 Published online by Cambridge University Press

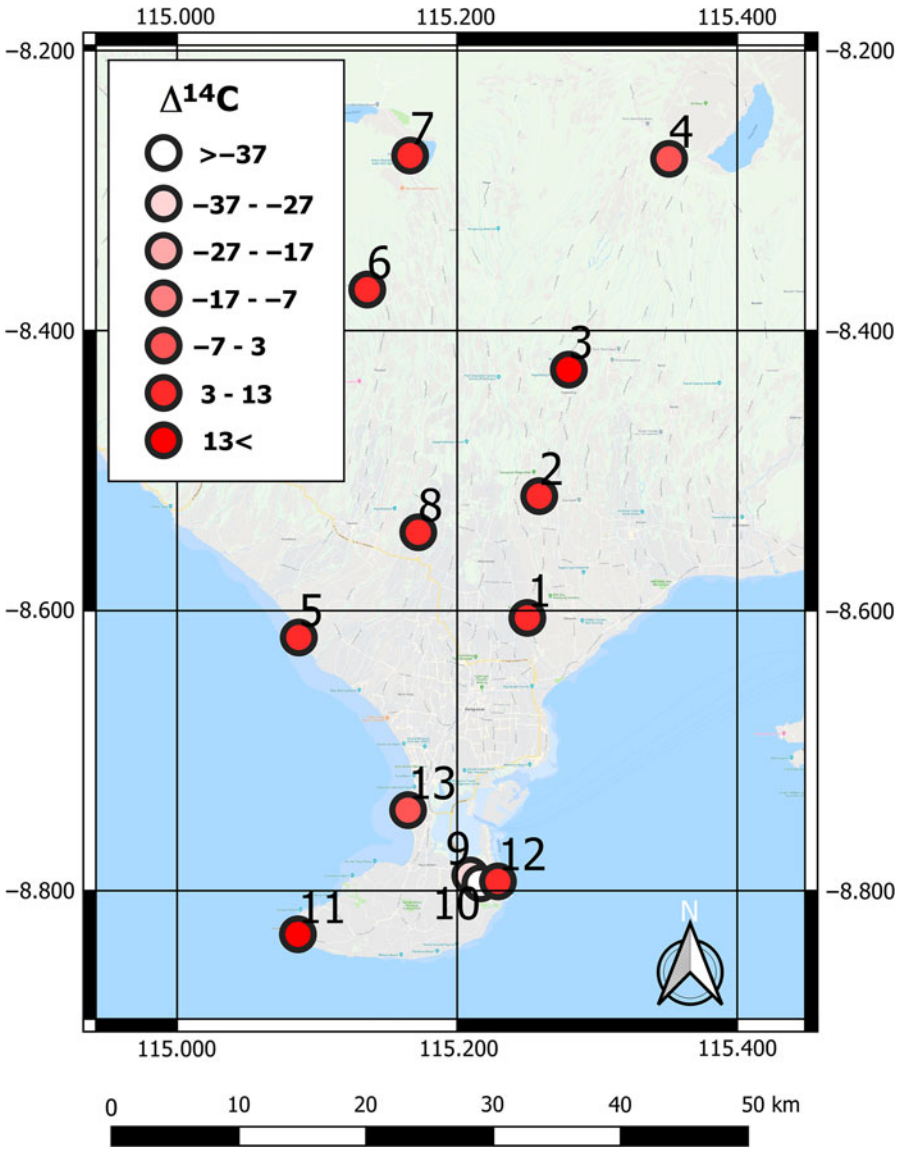

Figure 2 Map of the $\Delta^{14}C$ results in Bali, Indonesia.

that vehicles' idling engines emit radiocarbon-free CO_2 in high concentration continuously at this point source. In this approach, the crossroads can be identified as local point sources of fossil-fuel derived CO_2. The second most polluted area is a crossroad as well, at the end of the motorway, a six-lane road, where the conditions are similar to the no. 9 sampling point. These areas are well shielded by buildings and concrete fences, which can regulate the mixing of the air by local winds. The urban background samples and materials from rice fields show generally higher than 5‰ $\Delta^{14}C$ data (from 7.5 ± 4.6‰ to 18.2 ± 4.6‰). The 13 $\Delta^{14}C$ data points show that the radiocarbon concentration of air in most parts of Bali island is not so depleted.

https://doi.org/10.1017/RDC.2019.113 Published online by Cambridge University Press

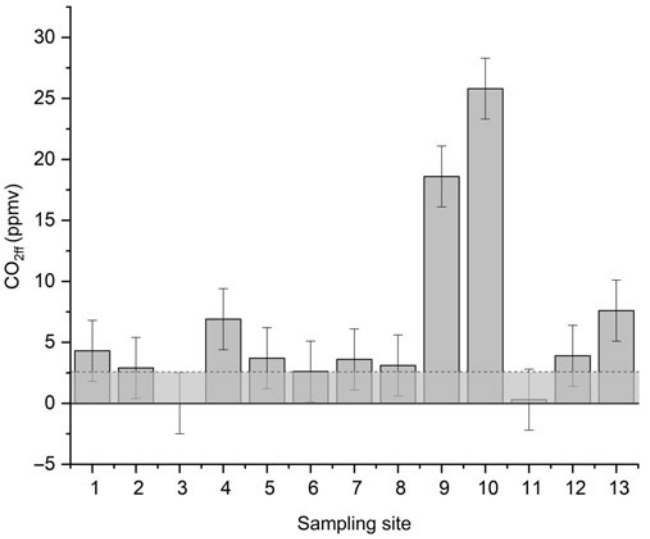

Figure 3 Fossil-fuel component (CO_{2ff}) using radiocarbon concentration in leaf samples. The transparent gray bar with dashed line indicates the error of the CO_{2ff} calculation.

The spatial distribution is given in Figure 2 and shows that the most depleted area is the densely populated southern region where local urban and tourist activity causes heavy traffic. The radiocarbon-free CO_2, mainly due to vehicular traffic, can dilute the local radiocarbon concentration in the frequented area. These data show that the Suess effect is observable on a local scale in a less industrialized region such as Bali as well. Close to Mount Batur, in a volcanic caldera (sampling point no. 4) there is no clearly observable radiocarbon depletion, the relatively lower $\Delta^{14}C$ data (0.9 ± 4.5‰) is presumably a consequence of the effect of tourist traffic in the nearby parking places, but cannot be clearly attributed as volcanic or magmatic CO_2 emission. Our data shows that the $\Delta^{14}C$ level is a little higher than zero ‰ in this equatorial, tropical region. It seems the declining radiocarbon bomb-peak is close to the preindustrial level. The fossil-fuel contribution to the local environment varies between 0.3 and 25.8 ppmv compared to the local background sample (Figure 3).

As shown by the $\Delta^{14}C$ data, sampling sites no. 9 and 10 are the most fossil-carbon loaded regions. These sites have dense traffic every day all year long, which causes high local fossil fuel originated CO_2 emission by fuel burning and exhaust. The other 10 samples show that the rest of the island is less affected by fossil carbon, with an average CO_{2ff} is 6.4 ± 7.5 ppmv.

CONCLUSION

In this study, evergreen woody plant samples were successfully used to detect a local Suess effect in Bali, Indonesia. There was a clear radiocarbon depletion in urban vegetation, in two cases where the radiocarbon-free CO_2 emission sources are the vehicles. At these crowded crossroads in a densely populated area, the local $\Delta^{14}C$ levels in the vegetation sampled were -28.2 ± 4.4‰ and -46 ± 4.3‰, compared to the highest data from a rice field, 18.2 ± 4.6‰. The spatial distribution shows that the radiocarbon level in the coastal area is not depleted and the Suess effect is observed only at the urbanized part of the island in

https://doi.org/10.1017/RDC.2019.113 Published online by Cambridge University Press

densely populated areas. Our data shows that the CO_2 concentration in densely populated areas can be 25 ppm more than annual global average CO_2 concentration, and the contribution of fossil sources can be 6% in the urban vegetation. Our data is comparable with other studies; the highest fossil contribution in this study is close to the winter seasonal value, 27.2 ppmv published in Kuc and Zimnoch 1998 (in Krakow). The recent dataset does not contain unusually high fossil carbon contributions, and there are higher measured data in a published study by Pawelczyk and Pazdur (2004), where the fossil contribution can be higher than 30 ppmv (in Krakow as well). In Quarta et al. (2007), the highest fossil carbon fraction is only 2.6% while our highest value is 6.3%. In our former study (Varga et al. 2019) the highest measured fossil carbon content was little higher, 9.6%, in a frequent urban area, at a busy crossroad in a Hungarian city, Debrecen. Our study shows that the radiocarbon level in vegetation, which reflects the atmospheric $^{14}CO_2$ concentration with a good approximation, is approaching the preindustrial level.

ACKOWLEDGMENTS

The research was supported by the European Union and the State of Hungary, co-financed by the European Regional Development Fund in the project of GINOP-2.3.2-15-2016-00009 "ICER".

REFERENCES

Alessio M, Anselmi S, Conforto L, Improta S, Manes F, Manfra L. 2002. Radiocarbon as a biomarker of urban pollution in leaves of evergreen species sampled in Rome and in rural areas (Lazio-Central Italy). Atmospheric Environment 36: 5405–5416

Baydoun R, Samad OEL, Nsouli B, Younes G. 2015. Measurement of ^{14}C content in leaves near a cement factory in Mount Lebanon. Radiocarbon 57(1):153–159

Bella F, Alessio M, Fratelli P. 1968. A determination of the half-life of ^{14}C. Il Nuovo Cimento 58B: 233–246

Berhanu TA, Szidat S, Brunner D, Satar E, Schanda R, Nyfeler P, Battaglia M, Steinbacher M, Hammer S, Leuenberger M. 2017. Estimation of the fossil fuel component in atmospheric CO_2 based on radiocarbon measurements at the Beromünster tall tower, Switzerland. Atmospheric Chemistry and Physics 17:10753–10766.

Buzinny M. 2006. Radioactive graphite dispersion in the environment in the vicinity of the Chernobyl Nuclear Power Plant. Radiocarbon 48(3): 451–458.

Cook AC, Hainswort LJ, Sorey ML, Evans WC, Southon JR. 2001. Radiocarbon studies of plant leaves and tree rings from Mammoth Mountain, CA: a long-term record of magmatic CO_2 release. Chemical Geology 177:117–131.

Ewers FW, Schmid R. 1981. Longecity of needle fascicles of *Pinus longaeva* (Bristlecone Pine) and other North American pines. Oecologia 51:107–115.

Fukumoto Y, Li X, Yasuda Y, Okamura M, Yamada K, Kashima K. 2015. The Holocene environmental changes in southern Indonesia reconstructed from highland caldera lake sediment in Bali Island. Quaternary International 374:15–33l.

Graven HD 2015. Impact of fossil fuel emissions on atmospheric radiocarbon and various applications of radiocarbon over this century. Proceedings of the National Academy of Sciences of the United States of America 112(31):9542–9545.

Janovics R, Futó I, Molnár M. 2018. Sealed tube combustion method with MnO_2 for AMS ^{14}C measurement. Radiocarbon 60(5):1347–1355.

Janovics R, Kelemen DI, Kern Z, Kapitány S, Veres M, Jull AJT, Molnár M. 2016. Radiocarbon signal of a low and intermediate level radioactive waste disposal facility in nearby trees. Journal of Environmental Radioactivity 153:10–14.

Janovics R, Kern Z, Güttler D, Wacker L, Barnabás I, Molnár M. 2013. Radiocarbon impact on a nearby tree of a light-water VVER-type nuclear power plant, Paks, Hungary. Radiocarbon 55(2–3): 826–832.

Kuc T, Zimnoch M. 1998. Changes of the CO_2 sources and sink in polluted urban area (southern Poland) over las decade, deriving from the carbon isotope composition. Radiocarbon 40(1):417–423.

Levin I, Kromer B, Schmidt M, Sartorius H. 2003. A novel approach for independent budgeting of fossil fuel CO_2 over Europe by $^{14}CO_2$ observation. Geophysical Research Letters 30(23):2194.

Levin I, Naegler T, Kromer B, Diehl M, Francey RJ, Gomez-Pelaez AJ, Steele LP, Wagenbach D, Weller R, Worthy DE. 2010. Observations and modelling of the global distribution and long-term trend of atmospheric $^{14}CO_2$. Tellus B (62B):26–46

https://doi.org/10.1017/RDC.2019.113 Published online by Cambridge University Press

Major I, Haszpra L, Rinyu L, Futó I, Bihari Á, Hammer S, Molnár M. 2018. Temporal variation of atmospheric fossil and modern CO_2 excess at a Central European rural tower station between 2008 and 2014. Radiocarbon 60(5): 1285–1299.

McNeely R. 1994. Long-term environmental monitoring of ^{14}C levels in the Ottawa region. Environment International 20(5):675–679.

Molnár M, Janovics R, Major I, Orsovszki J, Gönczi R, Veres M, Leonard AG, Castle SM, Lange TE, Wacker L, Hajdas I, Jull AJT. 2013. Status report of the new AMS ^{14}C sample preparation lab of the Hertelendi Laboratory of Environmental Studies (Debrecen, Hungary). Radiocarbon 55(2–3):665–676.

National Oceanic and Atmospheric Administration (NOAA), Earth System Research Laboratory, Global Monitoring Division. 2019. Mauna Loa CO2 annual mean data. Dataset: ftp://aftp.cmdl.noaa.gov/products/trends/co2/co2_annmean_mlo.txt [accessed 12 June 2019].

Nydal R, Lövseth K. 1983. Tracing bomb ^{14}C in the atmosphere 1962–1980. Journal of Geophysical Research 88(6):3621–3642.

Pataki DE, Randerson TJ, Wang W, Herzenach MK, Grulke NE. 2010 The carbon isotopic composition of plants and soils as a biomarkers of pollution In: West JB, Bowen GJ, Dawson TE, Tu KP, editors. Isoscapes: Understanding movement, pattern, and process on Earth through isotope mapping. Dordrecht: Springer. p. 407–423.

Pawelczyk S, Pazdur A. 2004. Carbon isotopic composition of tree rings as a tool for biomonitoring CO_2 level. Radiocarbon 46(2): 701–719.

Pazdur A, Nakamura T, Pawelczyk S, Pawlyta J, Piotrowska N, Rakowski A, Sensula B, Szczepanek M. 2007. Carbon isotopes in tree rings: climate and the Suess effect interferences in the last 400 years. Radiocarbon 49(2):775–788.

Povinec P, Kwong L.L.W, Kaizer J, Molnár M, Nies H, Palcsu L, Papp L, Pham M.K, Jean-Baptise P. 2017. Impact of the Fukushima accident on tritium, radiocarbon, and radiocesium levels in seawater of the western North Pacific Ocean: A comparison with pre-Fukushima situation. Journal of Environmental Radioactivity 166:56–66.

Quarta G, Rizzo G.A, D'elia M, Calcagnile L. 2007. Spatial and temporal reconstruction of the dispersion of anthropogenic fossil CO_2 by ^{14}C AMS measurements of plant material. Nuclear Instruments and Methods in Physics Research B 259:421–425.

Rahayu H, Haigh R, Amaratunga D. 2018 Strategic challenges in development planning for Denpasar City and the coastal urban agglomeration of Sabagita. Procedia Engineering 2012: 1347–1354.

Rakowski AZ. 2011. Radiocarbon method in monitoring of fossil fuel emission. Geochronometria 38(4):314–324.

Rinyu L, Molnár M, Major I, Nagy T, Veres M, Kimák Á, Wacker L, Synal H-A. 2013. Optimization of sealed tube graphitization method for environmental ^{14}C studies using MICADAS. Nuclear Instruments and Methods in Physics Research B 294:270–275.

Shore JS, Cook GT. 1995. The ^{14}C content of modern vegetation samples from the flanks of the Katla volcano, Southern Iceland. Radiocarbon 37(2):525–529.

Southon JR, Magana AL. 2010. A comparison of cellulose extraction and ABA pretreatment methods for AMS ^{14}C dating of ancient wood. Radiocarcon 52(2–3):1371–1379.

Stenström KE, Skog G, Georgiadou E, Grenberg J, Johansson A. 2011. A guide to radiocarbon units and calculations: Lund University [Sweden], Department of Physics, Division of Nuclear Physics Internal Report LUNFD6(NFFR-3111)/1-17/(2011).

Stuiver M, Polach H. 1977. Discussion: Reporting of ^{14}C data. Radiocarbon 19(3):355–363.

Suess HE. 1955. Radiocarbon concentration in modern wood. Science 122:415–417.

Synal HA, Stocker M, Suter M. 2007. MICADAS: A new compact radiocarbon AMS system. Nuclear Instruments and Methods in Physics Research B 259(1):7–13.

The International Plant Names Index (IPNI). 2019. Published on the Internet http://www.ipni.org [accessed 1 June 2019].

Varga T, Barnucz P, Major I, Lisztes-Szabó Zs, Jull AJT, László E, Pénzes J, Molnár M. 2019. Fossil carbon load in urban vegetation for Debrecen, Hungary. Radiocarbon 61(5). doi:10.1017/RDC.2019.81.

Varga T, Major I, Janovics R, Kurucz J, Veres M, Jull AJT, Péter M, Molnár M. 2018. High-precision biogenic fraction analyses of liquid fuels by ^{14}C AMS at HEKAL. Radiocarbon 60(5):1317–1325.

Wacker L, Christl M, Synal HA. 2010. Bats: A new tool for AMS data reduction. Nuclear Instruments and Methods in Physics Research B 268:976–979.